POLITECNICO DI TORINO
Repository ISTITUZIONALE

A numerical study on the dynamic pressure method for CO2 storage projects

Original
A numerical study on the dynamic pressure method for CO2 storage projects / Vespo, Vincenzo Sergio; Messori, Alessandro; Volonté, Giorgio; Musso, Guido. - In: E3S WEB OF CONFERENCES. - ISSN 2267-1242. - ELETTRONICO. - 205:(2022), p. 13016. (Intervento presentato al convegno 2nd International Conference on Energy Geotechnics (ICEGT 2020) tenutosi a La Jolla, California, USA nel April 10-13, 2022) [10.1051/e3sconf/202020513016].

Availability:
This version is available at: 11583/2950712 since: 2022-02-16T15:25:36Z

Publisher:
EDP Sciences

Published
DOI:10.1051/e3sconf/202020513016

Terms of use:

This article is made available under terms and conditions as specified in the corresponding bibliographic description in the repository

Publisher copyright

(Article begins on next page)

12 October 2024

A numerical study on the dynamic pressure method for CO_2 storage projects

Vincenzo Sergio Vespo[1], Alessandro Messori[2], Giorgio Volonté[2] and *Guido Musso*[1]

[1]Politecnico di Torino, Dipartimento di Ingegneria Strutturale, Edile e Geotecnica (DISEG), Corso Duca degli Abruzzi 24, 10129 Turin, Italy.
2Eni S.p.A.–Petroleum Engineering Laboratories (LAIP, Geomechanics), via Maritano 26, 20097 San Donato Milanese, Milan, Italy

1 Introduction

Carbon capture and storage is one of the possible actions to reduce CO2 concentration in the atmosphere and to contain the increase in the average temperature of the planet within two degrees centigrade, as required by the Paris climate agreements. Leakage may occur if the difference between the pressure of the injected CO_2 and the one of the brine saturating the caprock exceeds the threshold capillary pressure. Therefore, threshold pressure is a key parameter of the caprock sealing capacity. In the laboratory, a direct determination of the threshold pressure is obtained by forcing the non-wetting fluid into the brine saturated sample. The water pressure is maintained constant at the sample outlet, whereas the pressure of the non-wetting fluid is increased through steps at the inlet. A two-phase flow establishes once the imposed overpressure is higher than the threshold pressure. If the pressure steps are adequately small, an accurate evaluation of the threshold pressure is obtained however, because of the low permeability of the caprocks, this method is extremely time consuming. Several direct methods have been proposed in the last 20 years for faster characterization (Wu et al., 2020), among them the dynamic threshold pressure method. A numerical study was carried out with the FEM code COMSOL Multiphysics®, with the purpose of supporting the interpretation of the experimental results of one of them.

2 Dynamic Threshold Pressure Method

In the dynamic threshold pressure method, the non-wetting fluid is injected into the water saturated sample with a constant pressure that is higher than the threshold p^*_c value (Egermann et al., 2006). Before the experiment, water is also filled in the inlet tubing and gas is then charged to push the water into the sample, so determining the sample intrinsic permeability k_{int}. Water flow rate is recorded in the downstream side. As soon as CO_2 gets to the inlet face of the sample, a significant decrease of the water flow rate is recorded due to the capillary pressure jump at the non-wetting phase front. This jump is due to the start of two-phase flow. According to the method the pressure drop in the water-saturated region is:

(1) $\Delta p_w = \mu_w L Q_w^{eff} / \left(k_{int} A\right)$

where Q^{eff}_w is downstream brine flow rate, μ_w is the viscosity of water, L is the sample length, A is the sample cross-sectional. The estimated threshold capillary is then p°_c, evaluated as:

(2) $p_c^\circ = \Delta p_t - \Delta p_w$

where Δp_t is the constant overall pressure drop, above p^*_c, across the sample.

Numerical model

To simulate the dynamic method, the mass balance equations of water and CO_2 (non-wetting phase) were considered:

(3)

$$-C_{p,w}\frac{\partial\left(p_{nw}-p_w\right)}{\partial t}+\nabla\cdot\left[-\frac{k_{int}k_{r,w}}{\mu_w}\left(\nabla p_w+\rho_w g\nabla z\right)\right]=0$$

$$C_{p,w}\frac{\partial\left(p_{nw}-p_w\right)}{\partial t}+\nabla\cdot\left[-\frac{k_{int}k_{r,nw}}{\mu_{nw}}\left(\nabla p_{nw}+\rho_{nw} g\nabla z\right)\right]=0$$

where k_r is the relative permeability (a function of the saturation for a given fluid, in this model expressed according to van Genuchten, 1980), ρ is the fluid density. $C_{p,w}$ is the specific capacity of the wetting phase, which depends on changes in the effective saturation $S_{e,w}$ (in this model expressed according to van Genuchten, 1980) with respect to the capillary pressure as: $C_{p,w} = -\phi\left(\partial S_{e,w} / \partial p_c\right)$ where ϕ is the porosity of the porous medium, p_c is the capillary pressure ($p_c = p_{nw} - p_w$). Boundary conditions have been chosen to reproduce laboratory tests. Regarding the wetting fluid, the inlet boundary was set to be impervious, while a constant backpressure was imposed at the outlet. As for the non-wetting fluid, a constant pressure higher than the threshold pressure was set at the inlet boundary, while a no-flow conditions was imposed at the outlet. The expected response of an 80 mm high cylindrical specimen of clay shale was simulated. To observe the effect that the

* Corresponding author: vincenzosergio.vespo@polito.it

© The Authors, published by EDP Sciences. This is an open access article distributed under the terms of the Creative Commons Attribution License 4.0 (http://creativecommons.org/licenses/by/4.0/).

value of the applied non-wetting pressure has on the results and on the p°_c determination, a parametric study was carried out.

Table 1. Material parameters

k_{int} (m^2)	μ_w (Pa·s)	μ_{CO2} (Pa·s)	p^*_c (MPa)	van Genuchten parameters for water retention curve		
				α (MPa^{-1})	n	m
$5\cdot10^{-20}$	0.001	1.465	25	0.006	1.3	1.8

Figure 1 plots the numerical brine production curves for three different injection pressures. Accordingly with Egermann et al. (2006), a slope break is obtained in all cases when the CO_2 reaches the inlet of the specimen (10 hours from the start of these simulations) and it is more pronounced when the injection pressure is close to the threshold pressure. Figure 2 shows the threshold pressure determined for each instant of time by means of eq. (2). The results suggest a certain overestimation of the thresold pressure, which increases with determination time and applied CO_2 pressure. Figure 3 shows the predicted evolution of the maximum pressure (among the non-wetting and the wetting fluid) at different locations along the specimen. As the non wetting fluid approaches, and flows beyond the selected point, the pressure builds up. This pressure increase occurs along a time span which depends on the position along the specimen. Its value is relatively close to p^*_c near the inlet and decreases along the specimen.

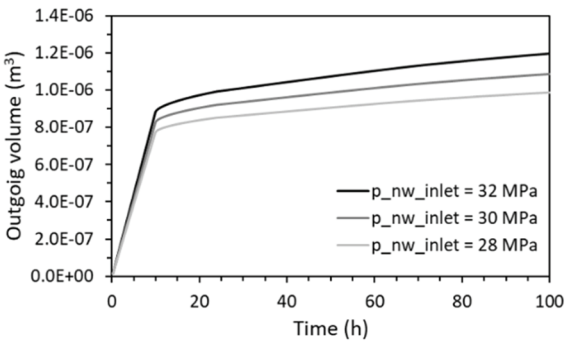

Fig. 1. Water outgoing volume vs. time for different injection pressures

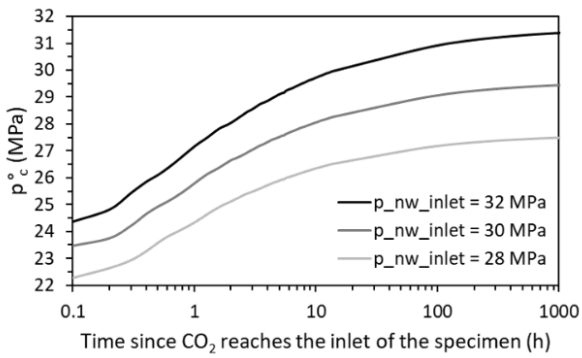

Fig. 2. Threshold pressure vs. determination time and injection pressures

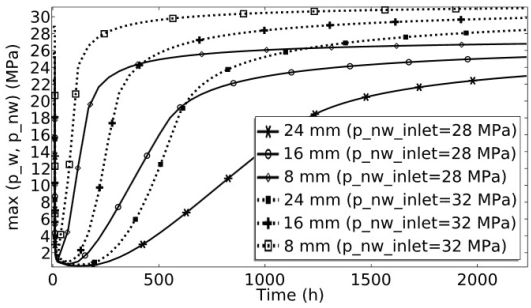

Fig. 3. Pressure evolution over time in different positions

References

1. Egermann, P., Lombard, J.M., Bretonnier, P. (2006). "A fast and accurate method to measure threshold capillary pressure of caprocks under representative conditions." Int. Symp. of the society of core analysts, Norway 12-16 September
2. van Genuchten, M. T. T. (1980). "A closed-form equation for predicting the hydraulic conductivity of unsaturated Soils." Soil Sci. Soc. Am. J., 44, 892–898.
3. Wu, T., Pan, Z., Connell, L.D., Liu, B., Fu, X., Xue, Z. (2020). "Gas threshold pressure of tight rocks: A review of experimental methods and data." J. of Natural Gas Science and Eng., 81, 103408